



UNIVERSITY OF LEEDS

This is a repository copy of *Intracellular Hg(0) Oxidation in Desulfovibrio desulfuricans ND132*.

White Rose Research Online URL for this paper:
<http://eprints.whiterose.ac.uk/109314/>

Version: Accepted Version

Article:

Wang, Y, Schaefer, JK, Mishra, B et al. (1 more author) (2016) Intracellular Hg(0) Oxidation in *Desulfovibrio desulfuricans* ND132. *Environmental Science and Technology*, 50 (20). pp. 11049-11056. ISSN 0013-936X

<https://doi.org/10.1021/acs.est.6b03299>

© 2016 American Chemical Society. This document is the Accepted Manuscript version of a Published Work that appeared in final form in *Environmental Science and Technology*, copyright © American Chemical Society after peer review and technical editing by the publisher. To access the final edited and published work see <https://doi.org/10.1021/acs.est.6b03299>. Uploaded in accordance with the publisher's self-archiving policy.

Reuse

Unless indicated otherwise, fulltext items are protected by copyright with all rights reserved. The copyright exception in section 29 of the Copyright, Designs and Patents Act 1988 allows the making of a single copy solely for the purpose of non-commercial research or private study within the limits of fair dealing. The publisher or other rights-holder may allow further reproduction and re-use of this version - refer to the White Rose Research Online record for this item. Where records identify the publisher as the copyright holder, users can verify any specific terms of use on the publisher's website.

Takedown

If you consider content in White Rose Research Online to be in breach of UK law, please notify us by emailing eprints@whiterose.ac.uk including the URL of the record and the reason for the withdrawal request.



eprints@whiterose.ac.uk
<https://eprints.whiterose.ac.uk/>

Intracellular Hg(0) oxidation in *Desulfovibrio desulfuricans* ND132

Yuwei Wang^a, Jeffra K. Schaefer^a, Bhoopesh Mishra^b, and Nathan Yee^{a,*}

^aDepartment of Environmental Sciences, Rutgers University, New Brunswick, New Jersey
08901, United States

^bDepartment of Physics, Illinois Institute of Technology, Chicago, IL 60616, USA

*Corresponding author: nyee@envsci.rutgers.edu

Submitted to Environmental Science & Technology

ABSTRACT

1
2
3
4
5
6
7
8
9
10
11
12
13
14
15
16
17
18
19
20
21
22
23

The disposal of elemental mercury [Hg(0)] wastes in mining and manufacturing areas have caused serious soil and groundwater contamination issues. Under anoxic conditions, certain anaerobic bacteria can oxidize dissolved elemental mercury and convert the oxidized Hg to neurotoxic methylmercury. In this study, we conducted experiments with the Hg-methylating bacterium *Desulfovibrio desulfuricans* ND132 to elucidate the role of cellular thiols in anaerobic Hg(0) oxidation. The concentrations of cell-surface and intracellular thiols were measured, and specific fractions of *D. desulfuricans* ND132 were examined for Hg(0) oxidation activity and analyzed with extended X-ray absorption fine structure (EXAFS) spectroscopy. The experimental data indicate that intracellular thiol concentrations are approximately six times higher than that of the cell wall. Cells reacted with a thiol-blocking reagent were severely impaired in Hg(0) oxidation activity. Spheroplasts lacking cell walls rapidly oxidized Hg(0) to Hg(II), while cell wall fragments exhibited low reactivity towards Hg(0). EXAFS analysis of spheroplast samples revealed that multiple different forms of Hg-thiols are produced by the Hg(0) oxidation reaction and that the local coordination environment of the oxidized Hg changes with reaction time. The results of this study indicate that Hg(0) oxidation in *D. desulfuricans* ND132 is an intracellular process that occurs by reaction with thiol-containing molecules.

24 INTRODUCTION

25

26 The fate and transport of mercury (Hg) in contaminated groundwater is strongly affected
27 by redox transformations.¹⁻³ Whereas oxidized ionic mercury [Hg(II)] binds strongly to natural
28 organic matter via complexation with thiol functional groups,^{4, 5} elemental mercury [Hg(0)] is
29 mobile in groundwater and can migrate horizontally over long distances through the unsaturated
30 zone as a volatile gas.^{6, 7} The conversion of Hg(0) to Hg(II) also affects the bioavailability of
31 mercury for bacterial uptake, the production of neurotoxic methylmercury [MeHg], and
32 subsequent bioaccumulation of MeHg in aquatic food webs.⁸⁻¹⁰ Understanding the
33 biogeochemical processes that control Hg(0) oxidation is particularly important for predicting
34 the formation of MeHg in industrial areas contaminated with large amounts of elemental
35 mercury, such as historic mining sites and nuclear weapon production facilities.¹¹⁻¹⁴

36 Certain anaerobic bacteria have been shown to produce MeHg from Hg(0) as the sole
37 mercury source.^{15, 16} A key step in the microbial conversion of dissolved elemental mercury to
38 methylmercury is the cellular oxidation of Hg(0) to Hg(II).¹⁷ The Hg-methylating bacterium
39 *Desulfovibrio desulfuricans* ND132 oxidizes dissolved elemental mercury to Hg(II) and the
40 oxidized Hg(II) covalently bonds to cellular functional groups.¹⁵ *Geobacter sulfurreducens* PCA
41 can also convert Hg(0) to Hg(II) but requires either high cell concentrations or the addition of
42 thiol compounds in its growth medium.^{16, 18} Because thiol functional groups in natural organic
43 matter have been shown to oxidize Hg(0) via oxidative complexation,^{19, 20} thiol-containing
44 molecules associated with bacterial cells may also be important for microbial Hg(0) oxidation.
45 Currently the role of cellular thiols, the location of Hg(0) oxidation, and the chemical forms of
46 oxidized mercury in Hg-methylating bacteria are poorly understood.

47 In this study, we conducted laboratory experiments to investigate thiol-mediated Hg(0)
48 oxidation in *D. desulfuricans* ND132. Cells were separated into spheroplasts (cells without cell
49 walls) and cell wall fragments, and experiments were conducted with the two fractions to better
50 understand cell-surface versus intracellular Hg(0) oxidation activity. The objectives of this study
51 were: (1) to quantify the concentration and distribution of thiol functional groups in *D.*
52 *desulfuricans* ND132; (2) to determine the cellular location of Hg(0) oxidation; and (3) to
53 characterize the chemical forms of oxidized mercury with EXAFS spectroscopy. The results of
54 this study provide new insights into Hg(0) uptake and complexation of Hg(II) in anaerobic Hg-
55 methylating bacteria.

56

57 MATERIALS AND METHODS

58

59 **Bacterial growth conditions.** *D. desulfuricans* ND132 was grown anaerobically (N₂
60 headspace) in a low sulfate medium modified from Gilmour et al.²¹ containing 25 mM pyruvate,
61 40 mM fumarate, 0.17 M NaCl, 6.4 mM NH₄Cl, 10 mM MOPS, 1.5 mM KH₂PO₄, 3.62 μM
62 FeCl₂, 6.7 mM KCl, 3.15 mM MgCl₂·6H₂O, 1.36 mM CaCl₂·2H₂O, 1 mL/L sulfate-free SL-7
63 trace metals,²² 0.5g/L yeast extract, and NaOH to adjust the pH to 7.2. Growth medium and
64 buffer solutions were rendered anoxic by boiling and bubbling with O₂-free N₂ gas. Cultures
65 were incubated statically at 30°C, harvested during mid-exponential phase (OD₆₀₀ ~ 0.25), and
66 washed twice with 0.5 mM MOPS buffer in an anaerobic glove box (Coy; 5:95 H₂:N₂ headspace)
67 before experimentation.

68

69 **Preparation of cell fractions.** *D. desulfuricans* ND132 cell walls (outmembrane and the
70 peptidoglycan layer) were removed by a procedure modified from a spheroplasts preparation
71 method for *Geobacter sulfurreducens*.²³ Briefly, cultures (200 mL) harvested at mid-exponential
72 phase were washed twice in an anaerobic glove box with a deoxygenated wash medium
73 containing 3.09 mM KH₂PO₄, 1.26 mM K₂HPO₄, 5.10mM KCl, 0.08M NaCl, 0.01 M MOPS,
74 350 mM sucrose at pH 6.8. The cells were then resuspended in 4 mL of 250 mM Tris buffer (pH
75 7.5) and 0.4 mL of 500 mM EDTA was added to chelate structural ions in the peptidoglycan
76 layer. After 1 min reaction with EDTA, 4 mL of 700 mM sucrose was added to the cell
77 suspension followed by the addition of lysozyme (75 mg). The cells were then incubated at 30 °C
78 from 1 minute to 24 hours. The optimum lysozyme incubation time was determined to be 6
79 hours. To induce osmotic shock, 8 mL of ultrapure water was then added to the suspension. The
80 resulting spheroplasts were immediately harvested by centrifugation at 20,000 g for 10 min. The
81 cell wall fragments in the supernatant were collected by ultracentrifugation at 177,500 g for 2
82 hours. Both the spheroplasts and cell wall fragments were then washed twice to remove residual
83 lysozyme from the incubation. Spheroplast formation was verified by fluorescence microscopy
84 in acridine orange-stained cells and quantified by direct counting method.²⁴ Over 90% of the
85 cells were converted to spheroplasts. Finally, spheroplast lysate was produced by resuspending
86 the spheroplasts in a hypotonic 0.5 mM MOPS buffer solution. Heat-treated spheroplast lysate
87 was prepared by heating the lysate at 80 °C for 10 min. Protein concentrations of intact cells,
88 spheroplasts and cell walls were measured by Bio-Rad protein assay.

89

90 **Determination of thiol functional groups.** The abundance of thiol functional groups was
91 determined by a florescence-labeling method using Thiol Fluorescent Probe 4 (TFP-4) [3-(7-

92 Hydroxy-2-oxo-2H-chromen-3-ylcarbonyl)acrylic acid methyl ester] (EMD Millipore
93 Corporation). TFP-4 is a cell-permeable fluorogenic probe that exhibits fluorescence when
94 reacted with reduced and solvent exposed R-SH compounds via an 1:1 Michael adduct
95 formation.^{25, 26} A 1 mM stock solution was prepared by dissolving TFP-4 in dimethyl sulfoxide
96 and diluting with acetonitrile. Experiments were conducted with spheroplasts and cell wall
97 fragments isolated from 7.4×10^8 cells/mL cell suspensions and re-suspended in 0.5 mM MOPS
98 buffer. The protein concentration of spheroplasts and cell wall fragments were 12 $\mu\text{g/mL}$ and 1.3
99 $\mu\text{g/mL}$, respectively. Whole cells experiments were conducted at a cell density of 7.7×10^8
100 cells/mL. TFP-4 titrations were performed by adding a known amount of the TFP-4 stock
101 solution to a set of sample and allowing the suspensions to react at room temperature for 2 h.
102 Fluorescence measurements were then made in 1 mL quartz cuvettes at an excitation wavelength
103 of 400 nm and peak emission intensity at 465 nm with a Molecular Devices Plate Reader. For
104 each set of samples, the TFP-4 titration resulted in a distinct inflection in the emission intensity
105 precisely at the point corresponding to the thiol concentration of the sample. The thiol content
106 per cell was determined with Avogadro's constant and normalizing the thiol concentration to cell
107 density.

108
109 **Hg(0) oxidation experiments.** The oxidation of Hg(0) by *D. desulfuricans* ND132 was
110 examined by exposing washed cell suspensions to a continuous source of Hg(0) gas. A drop of
111 liquid Hg(0) bead was placed in an uncapped HPLC vial inside of a 30 mL serum bottle wrapped
112 in aluminum foil and capped with a Teflon stopper. After purging the headspace of the bottle
113 with ultra-high purity N₂ for 25 min, the liquid Hg(0) bead was allowed to evaporate and
114 equilibrate with gas phase for 24 h. The liquid Hg(0) was added in excess and provided a

115 continuous supply of elemental mercury gas throughout the duration of the experiment. The
116 Hg(0) oxidation reaction was initiated by injecting 5 mL of cell suspension into the serum bottle
117 around the HPLC vial. The sample volume required for analysis was 300 μ L. The reactors were
118 shaken gently at 30 °C and sampled periodically for formation of non-purgeable Hg(II). At each
119 time point, cell suspension (0.5 mL) was removed from the reactor to an acid-cleaned I-Chem[®]
120 vial using a long needle and syringe, and the sample was purged immediately with ultra-high
121 purity N₂ for 2 min to remove unreacted Hg(0) gas. All samples were digested with 4 M nitric
122 acid and 0.2 M BrCl. Total non-purgeable Hg contents remaining in the samples were analyzed
123 by cold vapor atomic fluorescence spectrometry using a BrooksRand[®] MERX Total Mercury
124 Analytical System (EPA Method 1631) or cold vapor atomic absorption using a Leeman Labs
125 Hydra AA Mercury Analyzer (EPA Method 245.1).

126 Hg(0) oxidation experiments were repeated for TFP-4 treated cells, spheroplasts, and cell
127 wall fragments. TFP-4 treatment was carried out by suspending washed cells in deoxygenated
128 0.5 mM MOPS buffer and reacting the cells with 233 μ M TFP-4 to block cellular thiols. After 2
129 hours of reaction with TFP-4, cells were washed and resuspended with MOPS buffer, and then
130 injected into reactors for the Hg(0) oxidation experiment. Experiments with spheroplasts and cell
131 wall fragments were performed with cell suspensions at concentration of 8×10^8 cells/mL, where
132 the spheroplasts and cell wall fragments were separated by the protocol described above. The
133 protein concentration of spheroplasts and cell wall fragments were 16 μ g/mL and 2.3 μ g/mL,
134 respectively. The spheroplasts were suspended in a sucrose (350 mM) buffer to maintain isotonic
135 conditions throughout the experiment. Hg(0) oxidation experiments with cell wall fragments
136 were also conducted in the sucrose buffer to allow for direct comparison with the spheroplast
137 data.

138 **X-ray absorption spectroscopy.** Hg(0)-reacted *D. desulfuricans* ND132 spheroplasts were
139 analyzed using X-ray absorption spectroscopy. Spheroplasts reacted with Hg(0) were collected
140 from the reaction bottles and purged by ultra-high purity N₂ for 25 min and centrifuged at
141 12,000 g for 15 min. The pellets were then transferred to Teflon sample holder and sealed with
142 Kapton tape in an anaerobic chamber. The samples were placed in deoxygenated containers and
143 shipped to the Advanced Photon Source at Argonne National Laboratory for XAS analysis. Hg
144 L_{III}-edge EXAFS spectra were collected at beam line 13-ID-E, GeoSoilEnviroCARS, using Si (111)
145 monochromatic crystal with a 13 element germanium detector. Although sector 13-ID-E is capable
146 of focusing beam to 2 μm × 2 μm in vertical and horizontal directions, beam was defocused to
147 200 μm × 200 μm in vertical and horizontal directions and sample position was moved after every
148 2 scans to a fresh spot to mitigate beam induced chemistry. Spectra were collected under ambient
149 temperature, pressure, and an N₂ atmosphere. Energy calibration was performed such that the first
150 inflection points of Au foil and HgSn amalgam were assigned as 11919 and 12,284 eV respectively.
151 At least 15 spectra were collected for each sample to improve the signal-to-noise ratio. Spectral
152 features between scans were highly reproducible indicating minimal beam induced chemistry in
153 samples during data collection.

154 The data were analyzed by using the methods described in the UWXAFS package.²⁷ Data
155 processing and fitting were done with the programs ATHENA and ARTEMIS.²⁸ The data range
156 used for Fourier transformation of the k-space data was 2.5–8.5 Å⁻¹. The Hanning window function
157 was used with dk = 1.0 Å⁻¹. Fitting of each spectrum was performed in r-space, at 1.2-2.8 Å, with
158 multiple k-weighting (k¹, k², k³) unless otherwise stated. Lower χ^2 (reduced chi square) was used
159 as the criterion for inclusion of an additional shell in the shell-by-shell EXAFS fitting procedure.
160 Hg(0) and three Hg(II) standards [Hg-cysteine, Hg-(cysteine)₃, and Hg-acetate] were measured to

161 fingerprint Hg species in this study. Details of the shell-by-shell simultaneous fitting approach
162 used to model the EXAFS data are described elsewhere.²⁹

163

164 **RESULTS**

165

166 **Quantification of cellular thiols.** To determine the concentration of the intracellular thiols,
167 the cell wall of *D. desulfuricans* ND132 was removed and the spheroplast lysate was titrated
168 with the thiol-specific fluorescent probe TFP-4. The fluorescence emission increased steeply and
169 linearly until all the reduced thiols in the sample reacted with the fluorophore (Fig. 1A). After
170 stoichiometric reaction with the R-SH moieties, a decrease in slope in the titration curve was
171 observed. Best fit lines of the two linear regions of the titration curve showed an inflection point
172 at 12 μM which corresponded to the thiol concentration in the spheroplasts lysate sample. To
173 determine the concentration of thiol functional groups associated with the cell envelope, TFP-4
174 titrations were conducted with cell wall fragments. Similar to the spheroplast lysate experiment,
175 the slope of the titration curve increased steeply and linearly followed by a marked decrease in
176 fluorescence intensities at high TFP-4 concentrations (Fig. 1B). The titration curve for the cell
177 wall fragments showed an inflection point at 2 μM . Normalized to cell density, the thiol content
178 of the spheroplast (9.5×10^6 thiols/cell) was approximately 6 times higher than that of the cell
179 wall (1.7×10^6 thiols/cell). The combined thiols of the spheroplasts and cell walls was in close
180 agreement to the total thiol concentration determined for *D. desulfuricans* ND132 whole cells,
181 which exhibited an inflection point at 14 μM corresponding to a thiol number of 1.06×10^7
182 thiols/cell (Fig. 1C).

183

184 **Oxidation of Hg(0) to Hg(II).** We conducted experiments to determine the role of thiol-
185 containing molecules in Hg(0) oxidation by blocking the cellular sulfhydryl groups with TFP-4
186 before reacting the cells with Hg(0). TFP-4 conjugation with cellular thiols resulted in severe
187 impairment of Hg(0) oxidation activity (Fig. 2A). After 48 h, *D. desulfuricans* ND132 cells
188 formed 464 ppb Hg(II), while the TFP-4 treated cells produced only 60 ppb Hg(II). Over 85% in
189 Hg(0) oxidation activity was lost due to the blocking of cellular thiols with TFP-4.

190 To localize Hg(0) oxidation activity in the bacterial cells, experiments were conducted
191 with specific cell fractions of *D. desulfuricans* ND132. Spheroplasts lacking cell walls rapidly
192 oxidized Hg(0) with over 50 ppb of non-purgeable Hg formed in 6 h (Fig. 2B). Conversely, only
193 6 ppb was generated by cell wall fragments during this reaction time. The Hg(0) oxidized by
194 spheroplasts was approximately 8 times more than Hg(0) oxidized by cell walls. In order to
195 determine if intracellular components can account for the total Hg(0) oxidation activity observed
196 in whole cells, Hg(0) oxidation experiments were performed on lysed spheroplasts. Both whole
197 cells and spheroplast lysate exhibited similar Hg(0) oxidation capacity (Fig 2C). Heat-treated
198 spheroplast lysate retained Hg(0) oxidation activity (Fig. S1). Whole cells and spheroplasts
199 suspended in sucrose buffer showed similar Hg(0) oxidation activity, but slower reaction rates
200 were observed in sucrose buffer compared to MOPS buffer likely due Hg(0) diffusion and
201 solubility effects in the concentrated sucrose solution (Fig. S2). Interestingly, in MOPS buffer
202 the whole cells oxidized Hg(0) at a faster initial rate (8 ppb/h) compared to the spheroplast lysate
203 (6 ppb/h), suggesting that lysate conditions were sub-optimal relative to those maintained
204 natively by the cell (e.g. intact whole cells). This could be due to a number of factors including
205 the dispersal and dilution of sub-cellular components and/or the oxidation of thiol functional
206 groups upon exposure to the buffer. Despite this difference in initial oxidation rate, both

207 spheroplast lysates and whole cells oxidized a similar total amount of Hg(0) and there is no
208 statistical difference in the overall amount of non-purgeable Hg formed at the end of the
209 experiment.

210 **Chemical Speciation of Oxidized Hg.** X-ray absorption spectroscopy was performed to
211 examine the oxidation state and local binding environment of the spheroplast-associated Hg. The
212 Hg L_{III}-edge XANES spectra of the 1 h and 6 h samples were highly reproducible and showed
213 similarities with Hg-cysteine and Hg-(cysteine)₃ standards (Figures 3A and S1). The normalized
214 XANES spectra for spheroplast samples lack the pre-edge peak observed in the Hg-acetate
215 standard, suggesting that cell-associated Hg was not complexed to carboxyl functional groups.
216 First derivative of Hg XANES exhibited an energy separation (ΔE) between the first and second
217 energy peak for the spheroplast samples of 7.5 eV. The ΔE value was similar to that of Hg-cysteine
218 standard and significantly smaller than the ΔE value measured for the Hg-acetate standard (Fig.
219 S1b). These results indicate that the oxidized Hg is coordinated to sulfur (S) rather than oxygen
220 (O) atoms.

221 While no significant differences in the XANES spectra were observed between the 1 h and
222 6 h hours samples, the k^2 weighted $\chi(k)$ spectra showed a clear phase shift in the k^2 weighted $\chi(k)$
223 EXAFS oscillations between the 1 h and 6 h samples (Fig. 3B and S2). For the 6 h sample, the
224 phase of EXAFS oscillations shifted towards lower k values, which was manifested as longer bond
225 distance of the nearest neighbor atoms in the Fourier Transformed (FT) EXAFS data (Fig. 3C).
226 The Hg-S bond distance increased from 2.35 Å at 1 h to 2.43 Å at 6 h. The change in the Hg-S
227 bond distance was also evident from the real part of the FT EXAFS spectra (Fig. 3D). The Hg-S
228 bond distance for 1 h sample was slightly longer than the Hg-cysteine standard (2.30 Å) and the
229 Hg-S bond distance for 6 h sample was slightly shorter than the Hg-(cysteine)₃ standard (2.48 Å),

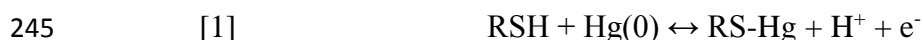
230 indicating there was a mixture of Hg-S species in the both samples. A shell-by-shell simultaneous
231 fitting approach was used to model the EXAFS data. Coordination numbers and bond distances
232 for the EXAFS modeling results are consistent with approximately 80% Hg-S₁ and 20% Hg-S₃ in
233 1 hour sample and 20% Hg-S₁ and 80% Hg-S₃ in 6 hour sample. Best fit values for EXAFS results
234 are shown in Table 1, and data and model fit are shown in Figure 4.

235

236 **DISCUSSION**

237

238 The experimental results presented in this study show that reduced thiols in *D.*
239 *desulfuricans* ND132 mediate Hg(0) oxidation. Inhibition of Hg(0) oxidation activity by the
240 blocking of sulfhydryl functional groups with the fluorophore TFP-4 indicates thiol functional
241 groups in biomolecules produced by *D. desulfuricans* ND132 chemically oxidize Hg(0) to
242 Hg(II). The oxidative process involves complexation of the thiols with Hg(0) followed by
243 electron transfer to an electron acceptor. This process is analogous to the redox reaction observed
244 with liquid Hg(0) drops reacted in thiol solutions:



246 Open circuit potential measurements have demonstrated that the adsorption of thiol compounds
247 onto hanging mercury drop electrodes leads to spontaneous Hg(0) oxidation.³⁰⁻³² Protons have
248 been suggested as the electron acceptor for this electrochemical process,³¹ with hydrogen (H₂) as
249 the reaction product. A similar mechanism has been proposed for Hg(0)_(aq) oxidation by low-
250 molecular-weight thiol compounds.^{20, 33} This oxidative mechanism would also be expected to
251 occur with biogenic thiol-containing molecules produced by *D. desulfuricans* ND132 in both
252 resting and metabolically-active cells.^{15, 16}

253 Hg(0) oxidation in *D. desulfuricans* ND132 is an intracellular process rather than a cell-
254 surface mediated reaction as previously suggested.^{16, 17} The experimental data implicate thiol-
255 containing molecules in either the cytoplasm or inner membrane as the reactive agents
256 responsible for Hg(0) oxidation (Fig. 2A). Because the intracellular thiol concentrations in *D.*
257 *desulfuricans* ND132 are approximately 6 times higher than the concentration of thiols on the
258 cell walls (Fig. 1), Hg(0) oxidation within the cell is significantly more favorable than in the cell
259 wall. Accordingly, our results showed that intracellular Hg(0) oxidation by spheroplasts was 8
260 times faster than cell surface Hg(0) oxidation (Fig. 2B). The fact that Hg(0) oxidation by
261 spheroplasts can account for all the Hg(0) oxidation activity observed in whole cells (Fig. 2C)
262 further supports the hypothesis that the oxidation of Hg(0) to Hg(II) is mediated by intracellular
263 reactions.

264 It is notable that the cell wall of *D. desulfuricans* ND132 exhibits very low reactivity
265 towards Hg(0) (Fig. 2B). Cell surface-associated thiols are reactive sites for Hg(II) adsorption in
266 gram negative bacteria,^{34, 35} and surface complexation reactions form thermodynamically stable
267 Hg-S complexes in the bacterial cell wall.³⁶ Although surface-associated thiols have been
268 proposed as the sites for Hg(0) oxidation in *G. sulfurreducens* PCA,^{16, 18} our data indicate the cell
269 surface thiols of *D. desulfuricans* ND132 do not play a central role in Hg(0) oxidation. It is
270 generally thought that Hg(0) can diffuse across bacterial membranes without undergoing
271 oxidation.³⁷ For example, during mercury detoxification Hg(II) by mercury-resistant bacteria,
272 Hg(II) is reduced to Hg(0) in the cytoplasm and dissolved gaseous mercury passively diffuses
273 out of the cell. The data presented in this study suggest that the reverse process can also occur,
274 whereby Hg(0) passively diffuses into the cell and undergoes oxidation to Hg(II) inside the
275 cytoplasm.

276 Hg(0) oxidation by *D. desulfuricans* ND132 is faster and occurs to a greater extent
277 compared to *G. sulfurreducens* PCA,¹⁶ and the difference in reactivity towards Hg(0) may be the
278 result of the relative cellular thiol concentration. Thiols are five hundred times more abundant in
279 *D. desulfuricans* ND132 than in *G. sulfurreducens*, where 2.1×10^4 thiols/cell were measured
280 using the maleimide-containing probe ThioGlo-1.³⁸ This large difference in the number of
281 reactive cellular thiols is expected to affect the kinetics and overall extent of Hg(0) oxidation.
282 Furthermore, Hu et al.¹⁶ showed that at low cell concentrations *G. sulfurreducens* PCA oxidizes
283 very little Hg(0) and requires the addition of exogenous cysteine to facilitate Hg(0) oxidation.
284 These observations suggest that biosynthesis of thiol-containing molecules and the flux between
285 oxidized and reduced thiol pools may be key controls on Hg(0) oxidation by anaerobic Hg-
286 methylating bacteria.

287 The thiol compounds in *D. desulfuricans* ND132 involved in Hg(0) oxidation have not
288 yet been identified. The most likely sites of reaction are the sulfhydryl functional groups
289 associated with cysteine residuals in solvent exposed proteins or small biomolecules. Oxidized
290 Hg has been shown to interact with thioredoxins³⁹ which are small cysteine containing proteins
291 produced by *D. desulfuricans* in response to oxidative stress.⁴⁰ Oxidative stress also induces the
292 expression of several thiol-specific peroxidases in *Desulfovibrio* including thiol-peroxidase,
293 bacterioferritin comigratory protein (BCP), and glutaredoxin.⁴¹ Conversely glutathione, which
294 occurs at high levels in aerobic bacteria, is not produced by *Desulfovibrio*⁴² and is unlikely to be
295 involved in Hg(0) oxidation unless assimilated from external sources.

296 The EXAFS analysis revealed that multiple forms of Hg-thiol complexes are produced
297 by intracellular Hg(0) oxidation in *D. desulfuricans* ND132. Linear combination fitting (LCF) of
298 the k^2 weighted $\chi(k)$ data using Hg-cysteine and Hg-(cysteine)₃ standards as end members

299 suggest a distribution of 70% Hg-S₁ and 30% Hg-S₃ in the 1 hour spheroplast sample, and 15%
300 Hg-S₁ and 85% Hg-S₃ in the 6 hour sample. These LCF estimates are in reasonably good
301 agreement with the shell-by-shell fitting results shown in Figure 4 and Table 1. A mixture of Hg-
302 S₁ and Hg-S₃ was also observed in the amplitude of the FT EXAFS data (Fig. S3). Destructive
303 interference of Hg-S₁ and Hg-S₃ signals, which are out of phase, resulted in much lower
304 amplitude for the FT EXAFS data for 1 h sample compared with the Hg-cysteine standard. The
305 chemical species Hg-S₂, which has a strong EXAFS signal, was not detected. On the other hand,
306 the amplitude for the FT EXAFS data for 6 h sample is similar to that of Hg-(cysteine)₃ standard.

307 Notably, the EXAFS analysis showed that the bond distance of Hg-S complexes changes
308 over time from 2.35 Å for the 1 h sample to 2.43 Å for the 6 h sample (Fig. 3B-D). This increase
309 in Hg-S bond distance is consistent with a modification of the Hg coordination environment from
310 1 S atom to 3 S atoms.⁴³ The Hg-S bond distance for the 1 hour sample is similar to Hg-thiol
311 bonds distances found in natural organic matter (2.34 Å) where Hg coordinates to a single sulfur
312 atom in a thiolated aromatic unit.⁴⁴ The 6 hour sample is dominated by a Hg-S₃ complex which
313 have been show to form in aqueous solutions when the cysteine ligand concentration exceeds
314 that of oxidized Hg by two fold.⁴⁵ Hg-S₄ complexes, which form in highly alkaline solutions,⁴⁶
315 are not likely to occur at physiological pH values of strain ND132. These findings indicate in the
316 presence of thiol-containing biomolecules, there is an evolution of the local coordination
317 environment of the intracellular oxidized Hg, with the stoichiometry of Hg-S bonding changing
318 from a predominately Hg-S₁ coordination environment to a more stable Hg-S₃ configuration with
319 increasing reaction time.

320 **Environmental Implications:** The experimental set up employed in our study resembles
321 the mercury contaminant situation at many industrial areas where a significant amount of the

322 elemental mercury waste persists in soils and sediments as liquid Hg beads.⁴⁷ Constant
323 evaporation and dissolution of the elemental mercury in our experiments mimic the continuous
324 supply of Hg that is leached into groundwater and becomes available for microbial interaction as
325 dissolved Hg(0). An example of this is the mercury contamination at Oak Ridge National
326 Laboratory (ORNL), Tennessee (USA) where members of Desulfovibrionaceae have been found
327 in groundwater monitoring wells at the Field Research Center of ORNL^{48, 49} adjacent to areas
328 where large amounts of elemental mercury were released into the environment.^{11, 12} The
329 oxidation of Hg(0) by Desulfovibrionaceae may represent one of the pathways of mercury
330 transformation at this site.

331 Intracellular Hg(0) oxidation in *D. desulfuricans* ND132 has important implications for
332 the production of methylmercury from dissolved elemental mercury. Because mercury
333 methylation is a cytosolic process, intracellular oxidation of Hg(0) to Hg(II) bypasses uptake
334 limitations for importing mercury into the cell and may provide a direct pathway for methylation.
335 Conversely, oxidized mercury associated with the cell wall can undergo desorption in the
336 presence of high affinity aqueous ligands. Low-molecular-weight thiol compounds that strongly
337 bind Hg are common in anoxic aquatic systems,⁵⁰ and the competitive binding of Hg(II) by
338 fulvic acids has been shown to decrease the extent of mercury adsorption onto cell walls of
339 *Bacillus subtilis*, *Shewanella oneidensis* MR-1, and *G. sulfurreducens* PCA bacterial species.³⁵
340 Furthermore in sulfidic waters, cell surface-associated Hg can partition into mineral forms and
341 precipitate as mercuric sulfide thus removing oxidized mercury from the cell. This is in contrast
342 to intracellular oxidized mercury which is not subject to desorption/precipitation processes. What
343 is not known is the reactivity of the intracellular oxidized mercury for methylation. An
344 interesting question is whether or not the Hg-S₁ and Hg-S₃ forms of intracellular mercury

345 detected in *D. desulfuricans* ND132 represent different bioavailable pools for methylation.
346 Understanding the reactive forms of intracellular mercury and the molecular reactions that
347 connect Hg(0) oxidation to MeHg production merit further investigation.

348

349 **ASSOCIATED CONTENT**

350

351 **Supporting Information.** Oxidation of Hg(0) to Hg(II) by heat-treated spheroplasts lysate in
352 MOPS buffer and by whole cells in sucrose buffer. XAS analysis of Hg(0)-reacted *D.*
353 *desulfuricans* ND132 spheroplasts including XANES spectra, k^2 -weighted EXAFS spectra, and
354 the magnitude and Fourier-transformed EXAFS spectra. The supporting information is available
355 free of charge on the ACS Publication website.

356

357 **AUTHOR INFORMATION**

358

359 **Corresponding Author.**

360 *N.Y. Phone: 848-932-5714; Email: nyee@envsci.rutgers.edu; Address: 14 College Farm Rd.,
361 New Brunswick NJ, 08901

362

363 **ACKNOWLEDGEMENTS**

364

365 This research was supported by the U.S. Department of Energy, Office of Science (BER) no.
366 DE-SC0007051. BM was supported by NSF (Earth Sciences) Geobiology and Low-Temperature
367 Geochemistry program (EAR-1424968). GeoSoilEnviroCARS is supported by the National
368 Science Foundation - Earth Sciences (EAR-0622171) and Department of Energy - Geosciences

369 (DE-FG02-94ER14466). Use of the Advanced Photon Source was supported by the U. S.
370 Department of Energy, Office of Science, Office of Basic Energy Sciences, under Contract No.
371 DE-AC02-06CH11357. Technical support from beam line personnel was provided by Tony
372 Lanzirotti and Matt Newville. We thank four anonymous reviewers for their insightful comments
373 that greatly improved the manuscript.

REFERENCES

- (1) Lamborg, C. H.; Kent, D. B.; Swarr, G. J.; Munson, K. M.; Kading, T.; O'Connor, A. E.; Fairchild, G. M.; LeBlanc, D. R.; Wiatrowski, H. A., Mercury speciation and mobilization in a wastewater-contaminated groundwater plume. *Environ. Sci. Technol.* **2013**, 47 (23), 13239-13249.
- (2) Julia, B. L.; et al. Occurrence and Mobility of Mercury in Groundwater. In *Current Perspectives in Contaminant Hydrology and Water Resource Sustainability*; Paul M Bradley; InTech: 2013; pp 117-149.
- (3) Richard, J.-H.; Bischoff, C.; Ahrens, C. G.; Biester, H., Mercury (II) reduction and co-precipitation of metallic mercury on hydrous ferric oxide in contaminated groundwater. *Sci. Total Environ.* **2016**, 539, 36-44.
- (4) Xia, K.; Skyllberg, U.; Blear, W.; Bloom, P.; Nater, E.; Helmke, P., X-ray absorption spectroscopic evidence for the complexation of Hg (II) by reduced sulfur in soil humic substances. *Environ. Sci. Technol.* **1999**, 33 (2), 257-261.
- (5) Ravichandran, M., Interactions between mercury and dissolved organic matter--a review. *Chemosphere* **2004**, 55 (3), 319-31.
- (6) Walvoord, M. A.; Andraski, B. J.; Krabbenhoft, D. P.; Striegl, R. G., Transport of elemental mercury in the unsaturated zone from a waste disposal site in an arid region. *Appl. Geochem.* **2008**, 23 (3), 572-583.
- (7) Bollen, A.; Wenke, A.; Biester, H., Mercury speciation analyses in HgCl₂-contaminated soils and groundwater--implications for risk assessment and remediation strategies. *Water Res.* **2008**, 42 (1-2), 91-100.
- (8) Morel, F. M.; Kraepiel, A. M.; Amyot, M., The chemical cycle and bioaccumulation of mercury. *Annu. Rev. Ecol. Syst.* **1998**, 29, 543-566.
- (9) Lin, C. C.; et al. Microbial transformations in the mercury cycle. In *Environmental Chemistry and Toxicology of Mercury*; Liu, G.; Cai, Y.; O'Driscoll, N.; John Wiley & Sons, Inc.: 2012, pp 155-191.
- (10) Hsu-Kim, H.; Kucharzyk, K. H.; Zhang, T.; Deshusses, M. A., Mechanisms regulating mercury bioavailability for methylating microorganisms in the aquatic environment: a critical review. *Environ. Sci. Technol.* **2013**, 47 (6), 2441-2456.

- (11) Brooks, S. C.; Southworth, G. R., History of mercury use and environmental contamination at the Oak Ridge Y-12 Plant. *Environ. Pollut.* **2011**, 159 (1), 219-228.
- (12) Miller, C. L.; Watson, D. B.; Lester, B. P.; Lowe, K. A.; Pierce, E. M.; Liang, L., Characterization of soils from an industrial complex contaminated with elemental mercury. *Environ. Res.* **2013**, 125, 20-29.
- (13) Lechler, P. J.; Miller, J. R.; Hsu, L.-C.; Desilets, M. O., Mercury mobility at the Carson River Superfund Site, west-central Nevada, USA: interpretation of mercury speciation data in mill tailings, soils, and sediments. *J. Geochem. Explor.* **1997**, 58 (2), 259-267.
- (14) Slowey, A. J.; Rytuba, J. J.; Brown, G. E., Speciation of mercury and mode of transport from placer gold mine tailings. *Environ. Sci. Technol.* **2005**, 39 (6), 1547-1554.
- (15) Colombo, M. J.; Ha, J.; Reinfelder, J. R.; Barkay, T.; Yee, N., Anaerobic oxidation of Hg(0) and methylmercury formation by *Desulfovibrio desulfuricans* ND132. *Geochim. Cosmochim. Acta* **2013**, 112, 166-177.
- (16) Hu, H.; Lin, H.; Zheng, W.; Tomanicek, S. J.; Johs, A.; Feng, X.; Elias, D. A.; Liang, L.; Gu, B., Oxidation and methylation of dissolved elemental mercury by anaerobic bacteria. *Nat. Geosci.* **2013**, 6 (9), 751-754.
- (17) Lin, H.; Hurt, R. A.; Johs, A.; Parks, J. M.; Morrell-Falvey, J. L.; Liang, L.; Elias, D. A.; Gu, B., Unexpected Effects of Gene Deletion on Interactions of Mercury with the Methylation-Deficient Mutant *ΔhgcAB*. *Environ. Sci. Technol. Lett.* **2014**, 1 (5), 271-276.
- (18) Lin, H.; Morrell-Falvey, J. L.; Rao, B.; Liang, L.; Gu, B., Coupled mercury-cell sorption, reduction, and oxidation on methylmercury production by *Geobacter Sulfurreducens* PCA. *Environ. Sci. Technol.* **2014**, 48 (20), 11969-76.
- (19) Gu, B.; Bian, Y.; Miller, C. L.; Dong, W.; Jiang, X.; Liang, L., Mercury reduction and complexation by natural organic matter in anoxic environments. *Proc. Natl. Acad. Sci. U.S.A.* **2011**, 108 (4), 1479-83.
- (20) Zheng, W.; Liang, L.; Gu, B., Mercury reduction and oxidation by reduced natural organic matter in anoxic environments. *Environ. Sci. Technol.* **2012**, 46 (1), 292-9.
- (21) Gilmour, C. C.; Elias, D. A.; Kucken, A. M.; Brown, S. D.; Palumbo, A. V.; Schadt, C. W.; Wall, J. D., Sulfate-reducing bacterium *Desulfovibrio desulfuricans* ND132 as a model for understanding bacterial mercury methylation. *Appl. Environ. Microbiol.* **2011**, 77 (12), 3938-51.

- (22) Widdel, F.; Pfennig, N., Sporulation and further nutritional characteristics of *Desulfotomaculum acetoxidans*. *Arch. Microbiol.* **1981**, 129 (5), 401-402.
- (23) Coppi, M. V.; O'Neil R, A.; Leang, C.; Kaufmann, F.; Methe, B. A.; Nevin, K. P.; Woodard, T. L.; Liu, A.; Lovley, D. R., Involvement of *Geobacter sulfurreducens* SfrAB in acetate metabolism rather than intracellular, respiration-linked Fe(III) citrate reduction. *Microbiology* **2007**, 153 (Pt 10), 3572-85.
- (24) Hobbie, J. E.; Daley, R. J.; Jasper, S., Use of Nucleopore filters for counting bacteria by fluorescence microscopy. *Appl. Environ. Microbiol.* **1977**, 33 (5), 1225-1228.
- (25) Yi, L.; Li, H.; Sun, L.; Liu, L.; Zhang, C.; Xi, Z., A Highly Sensitive Fluorescence Probe for Fast Thiol-Quantification Assay of Glutathione Reductase. *Angew. Chem. Int. Ed.* **2009**, 48 (22), 4034-4037.
- (26) Campuzano, I. D.; San Miguel, T.; Rowe, T.; Onea, D.; Cee, V. J.; Arvedson, T.; McCarter, J. D., High-Throughput Mass Spectrometric Analysis of Covalent Protein-Inhibitor Adducts for the Discovery of Irreversible Inhibitors A Complete Workflow. *J. Biomol. Screen* **2015**, 21 (2), 109-110.
- (27) Stern, E.; Newville, M.; Ravel, B.; Yacoby, Y., The UWXAFS analysis package: philosophy and details. *Physica. B: Condensed Matter* **1995**, 117-120.
- (28) Ravel, B.; Newville, M., ATHENA and ARTEMIS: interactive graphical data analysis using IFEFFIT. *Phys. Scripta* **2005**, 2005 (T115), 1007.
- (29) Mishra, B.; Boyanov, M.; Bunker, B. A.; Kelly, S. D.; Kemner, K. M.; Fein, J. B., High- and low-affinity binding sites for Cd on the bacterial cell walls of *Bacillus subtilis* and *Shewanella oneidensis*. *Geochim. Cosmochim. Acta* **2010**, 74 (15), 4219-4233.
- (30) Muskal, N.; Mandler, D., Thiol self-assembled monolayers on mercury surfaces: the adsorption and electrochemistry of ω -mercaptoalkanoic acids. *Electrochim. Acta* **1999**, 45 (4), 537-548.
- (31) Cohen-Atiya, M.; Mandler, D., Studying thiol adsorption on Au, Ag and Hg surfaces by potentiometric measurements. *J. Electroanal. Chem.* 2003, 550, 267-276.
- (32) Mandler, D.; Kraus-Ophir, S., Self-assembled monolayers (SAMs) for electrochemical sensing. *J. Solid State Electrochem.* **2011**, 15 (7-8), 1535-1558.

- (33) Zheng, W.; Lin, H.; Mann, B. F.; Liang, L.; Gu, B., Oxidation of dissolved elemental mercury by thiol compounds under anoxic conditions. *Environ. Sci. Technol.* **2013**, *47* (22), 12827-34.
- (34) Hu, H.; Lin, H.; Zheng, W.; Rao, B.; Feng, X.; Liang, L.; Elias, D. A.; Gu, B., Mercury reduction and cell-surface adsorption by *Geobacter sulfurreducens* PCA. *Environ. Sci. Technol.* **2013**, *47* (19), 10922-30.
- (35) Dunham-Cheatham, S.; Mishra, B.; Myneni, S.; Fein, J. B., The effect of natural organic matter on the adsorption of mercury to bacterial cells. *Geochim. Cosmochim. Acta* **2015**, *150*, 1-10.
- (36) Mishra, B.; O'Loughlin, E. J.; Boyanov, M. I.; Kemner, K. M., Binding of Hg(II) to high-affinity sites on bacteria inhibits reduction to Hg(0) by mixed FeII/III phases. *Environ. Sci. Technol.* **2011**, *45* (22), 9597-603.
- (37) Barkay, T.; Miller, S. M.; Summers, A. O., Bacterial mercury resistance from atoms to ecosystems. *FEMS Microbiol. Rev.* **2003**, *27* (2-3), 355-384.
- (38) Rao, B.; Simpson, C.; Lin, H.; Liang, L.; Gu, B., Determination of thiol functional groups on bacteria and natural organic matter in environmental systems. *Talanta* **2014**, *119*, 240-7.
- (39) Wang, Y.; Robison, T.; Wiatrowski, H., The impact of ionic mercury on antioxidant defenses in two mercury-sensitive anaerobic bacteria. *Biometals* **2013**, *26* (6), 1023-1031.
- (40) Sarin, R.; Sharma, Y. D., Thioredoxin system in obligate anaerobe *Desulfovibrio desulfuricans*: Identification and characterization of a novel thioredoxin 2. *Gene* **2006**, *376* (1), 107-115.
- (41) Fournier, M.; Aubert, C.; Dermoun, Z.; Durand, M.-C.; Moinier, D.; Dolla, A., Response of the anaerobe *Desulfovibrio vulgaris* Hildenborough to oxidative conditions: proteome and transcript analysis. *Biochimie.* **2006**, *88* (1), 85-94.
- (42) Fahey, R.; Brown, W.; Adams, W.; Worsham, M., Occurrence of glutathione in bacteria. *J. Bacteriol.* **1978**, *133* (3), 1126-1129.
- (43) Manceau, A.; Nagy, K. L., Relationships between Hg(II)-S bond distance and Hg(II) coordination in thiolates. *Dalton Trans.* **2008**, (11), 1421-5.
- (44) Nagy, K. L.; Manceau, A.; Gasper, J. D.; Ryan, J. N.; Aiken, G. R., Metallothionein-like multinuclear clusters of mercury (II) and sulfur in peat. *Environ. Sci. Technol.* **2011**, *45* (17), 7298-7306.

- (45) Cheesman, B. V.; Arnold, A. P.; Rabenstein, D. L., Nuclear magnetic resonance studies of the solution chemistry of metal complexes. 25. Hg (thiol)₃ complexes and Hg (II)-thiol ligand exchange kinetics. *J. Am. Chem. Soc.* **1988**, 110 (19), 6359-6364.
- (46) Jalilehvand, F.; Leung, B. O.; Izadifard, M.; Damian, E., Mercury (II) cysteine complexes in alkaline aqueous solution. *Inorg. Chem.* **2006**, 45 (1), 66-73.
- (47) Liang, L.; Watson, D. B.; Miller, C.; Howe, J.; He, F.; Pierce, E., The fate of mercury at a contaminated site. Goldschmidt Conference, Montreal, Canada, 2012.
- (48) Hwang, C.; Wu, W.; Gentry, T. J.; Carley, J.; Corbin, G. A.; Carroll, S. L.; Watson, D. B.; Jardine, P. M.; Zhou, J.; Criddle, C. S., Bacterial community succession during in situ uranium bioremediation: spatial similarities along controlled flow paths. *ISME J.* **2009**, 3 (1), 47-64.
- (49) Gihring, T. M.; Zhang, G.; Brandt, C. C.; Brooks, S. C.; Campbell, J. H.; Carroll, S.; Criddle, C. S.; Green, S. J.; Jardine, P.; Kostka, J. E.; Lowe, K.; Mehlhorn, T. L.; Overholt, W.; Watson, D. B.; Yang, Z.; Wu, W. M.; Schadt, C. W., A limited microbial consortium is responsible for extended bioreduction of uranium in a contaminated aquifer. *Appl. Environ. Microbiol.* **2011**, 77 (17), 5955-65.
- (50) Xia, K.; Weesner, F.; Blears, W.; Helmke, P.; Bloom, P.; Skylberg, U., XANES studies of oxidation states of sulfur in aquatic and soil humic substances. *Soil Sci. Soc. Am. J.* **1998**, 62 (5), 1240-1246.

Table 1: Best fit values for EXAFS analysis of spheroplast samples.

Sample	path	CN	R (Å)	$\sigma^2 \cdot 10^{-3} (\text{Å}^{-1})$	ΔE (eV)
ND132; 1 hr	Hg-S	1.36 ± 0.24	2.35 ± 0.01	2.5 ± 1.5	-1.46 ± 1.1
ND132; 6 hrs	Hg-S	2.48 ± 0.43	2.43 ± 0.01	8.1 ± 2.3	-1.46 ± 1.1

Note: CN, R and σ^2 represent coordination number, distance, and variance, respectively.

Figure 1. Fluorescence intensities of *D. desulfuricans* ND132 reacted with Thiol Fluorescent Probe IV (TFP-4). (A) Spheroplast lysate (open circles); (B) Cell wall fragments (open squares); (C) ND132 whole cells (closed circles). Each data point represents an individual experiment conducted in the same day.

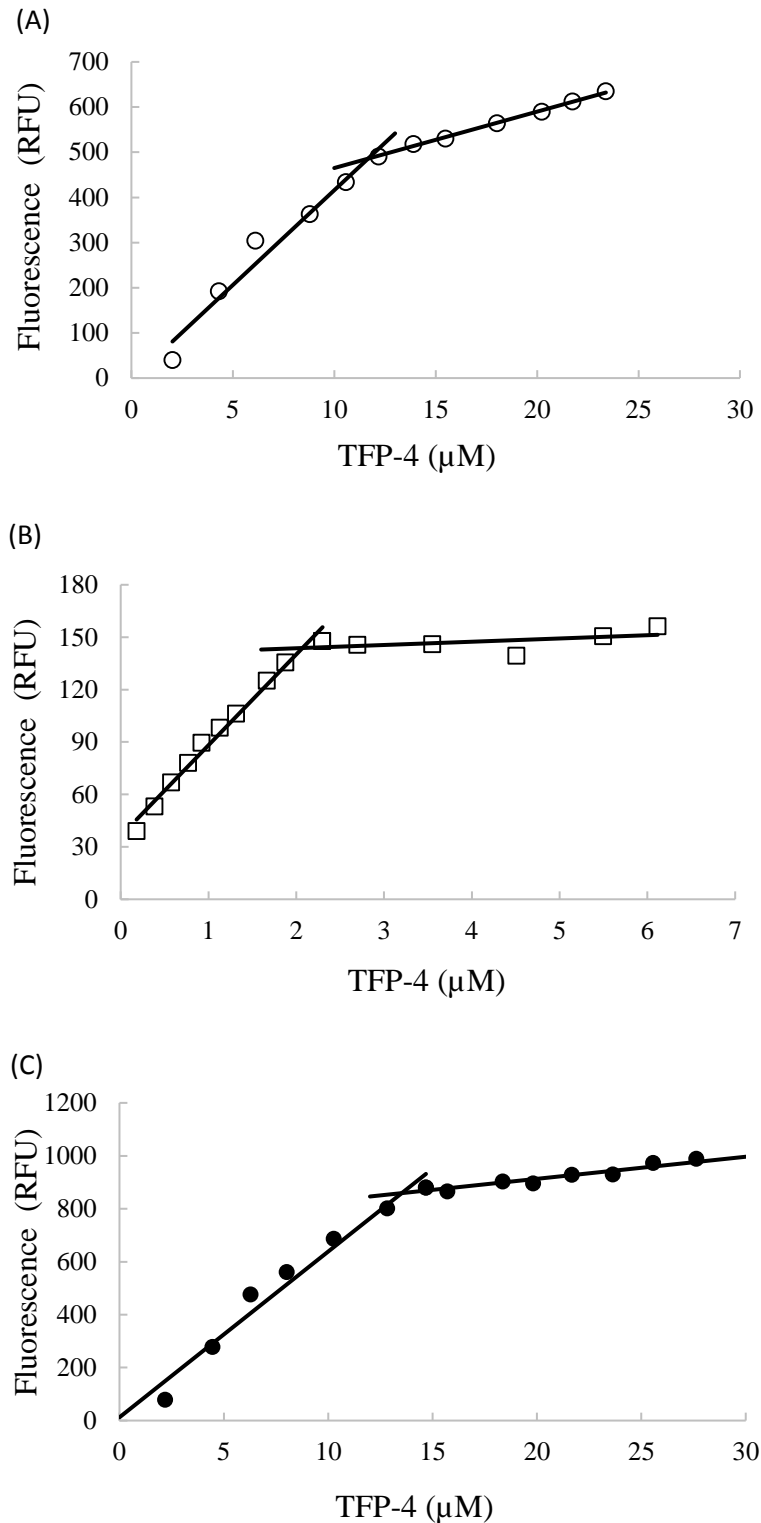


Figure 2. Oxidation of Hg(0) to Hg(II) by *D. desulfuricans* ND132. (A) Production of Hg(II) by *D. desulfuricans* ND132 whole cells (closed circles) and TFP-4 treated whole cells (closed triangle) in MOPS buffer. (B) Hg(II) formed by spheroplasts (open circles) and cell walls (open squares) in sucrose buffer. (C) Formation of Hg(II) by whole cells (closed circles) and spheroplasts lysate suspensions (open circles). All experiments were conducted with an initial cell concentration of 8×10^8 cells/mL. Points and error bars represent the means and standard deviations of triplicate experiments.

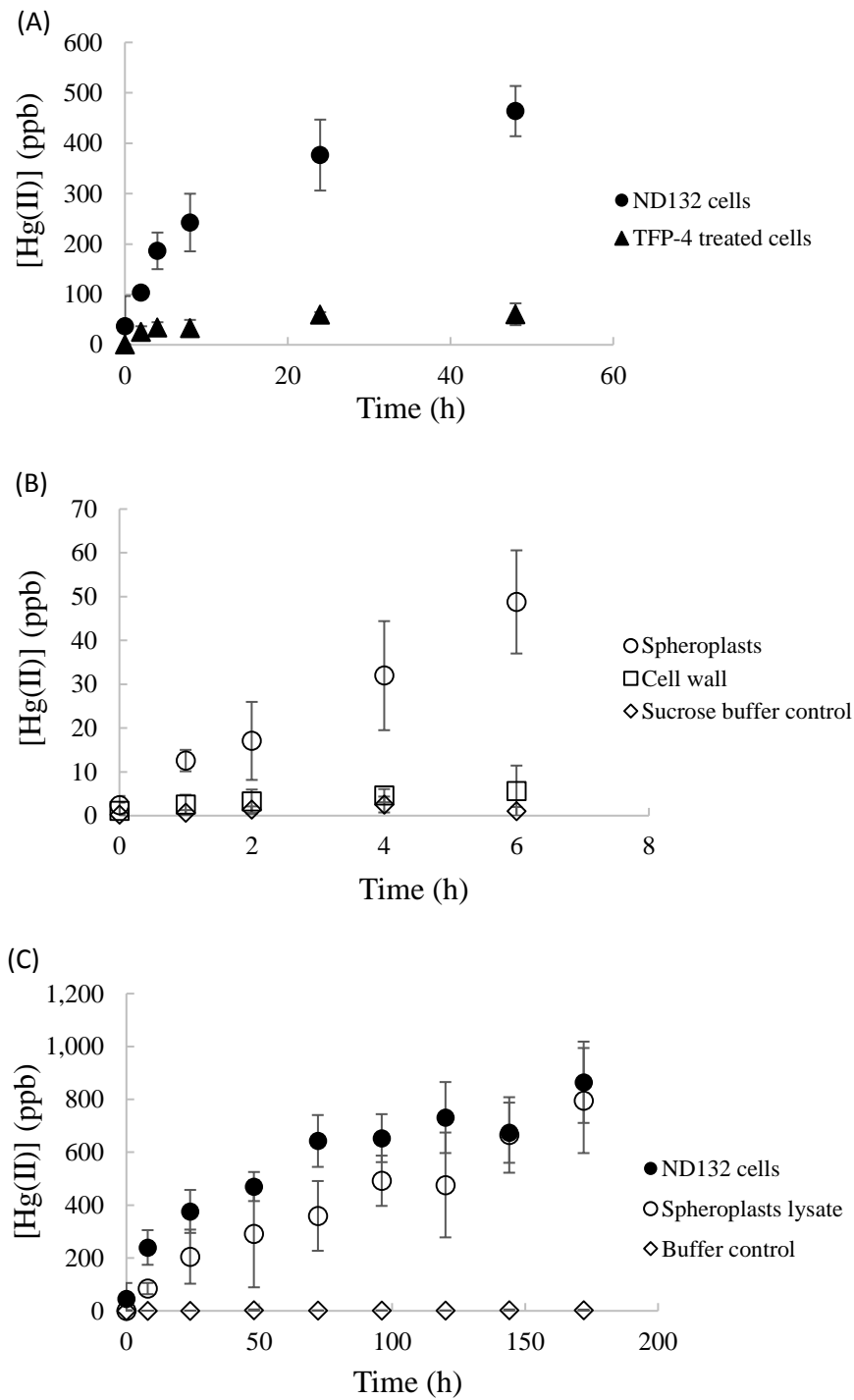


Figure 3. Structure characterization of Hg(0)-reacted *D. desulfuricans* ND132 spheroplasts by X-ray absorption spectroscopy (XAS) analysis at the Hg LIII-edge. (A) XANES spectra of spheroplasts samples collected at 1 h (black curve) and 6 h (red curve). The inset shows the first derivatives of the XANES spectra. (B) The k^2 -weighted EXAFS spectra in k -space collected on the 1 h and 6 h spheroplasts samples. (C) Magnitude of the Fourier-transformed EXAFS spectra in R -space of 1 h and 6 h spheroplasts samples. (D) Real part of Fourier-transformed EXAFS spectra.

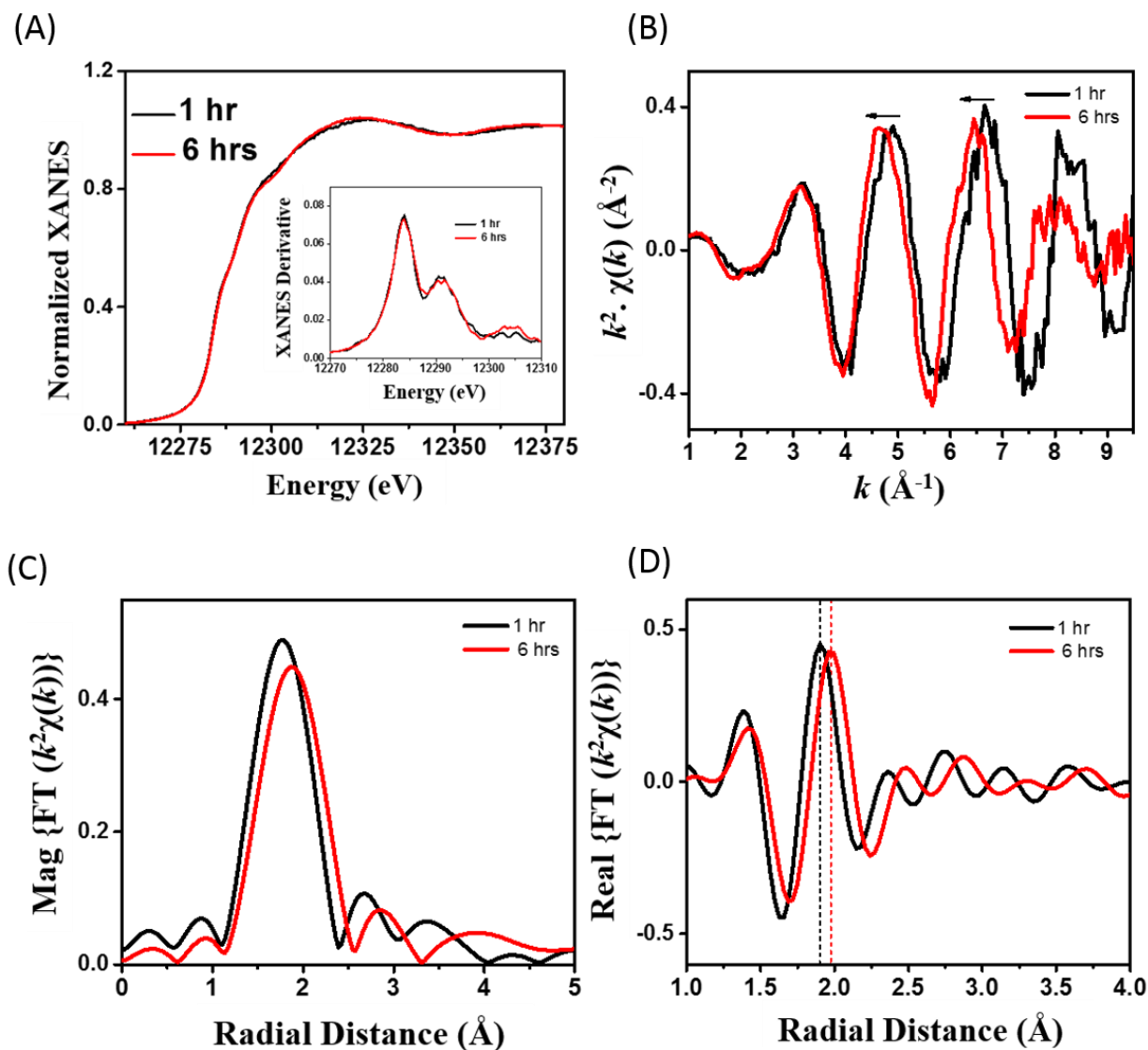
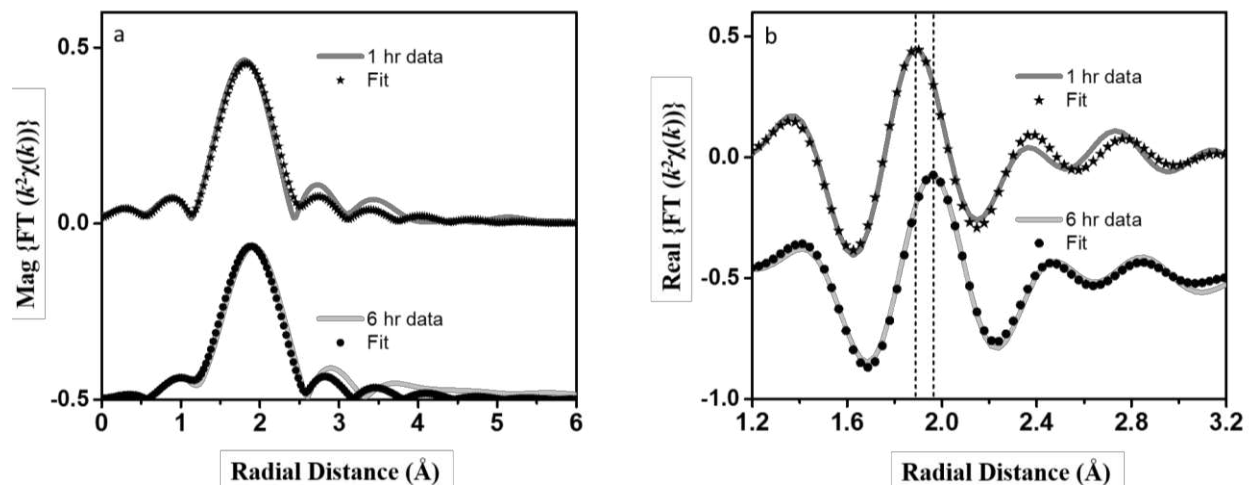


Figure 4: EXAFS data and fit for the (a) magnitude and (b) real part of the Fourier-transformed EXAFS spectra in R-space of 1 h and 6 h spheroplasts samples.



SUPPORTING INFORMATION

Intracellular Hg(0) oxidation in *Desulfovibrio desulfuricans* ND132

Yuwei Wang^a, Jeffra K. Schaefer^a, Bhoopesh Mishra^b, and Nathan Yee^{a,*}

^aDepartment of Environmental Sciences, Rutgers University, New Brunswick, New Jersey
08901, United States

^bDepartment of Physics, Illinois Institute of Technology, Chicago, IL 60616, USA

*Corresponding author: nyee@envsci.rutgers.edu

Table of Contents

Fig. S1	Oxidation of Hg(0) to Hg(II) by <i>D. desulfuricans</i> ND132 spheroplasts lysate and heat-treated spheroplasts lysate	S2
Fig. S2	Oxidation of Hg(0) to Hg(II) by <i>D. desulfuricans</i> ND132 whole cells and spheroplasts in sucrose buffer	S3
Fig. S3	XANES spectra of Hg(0)-reacted <i>D. desulfuricans</i> ND132 spheroplasts	S4
Fig. S4	The k^2 -weighted EXAFS spectra in k -space collected on spheroplasts samples and Hg-(cysteine) _n standards.	S5
Fig. S5	Magnitude and real part of the Fourier-transformed EXAFS spectra in R -space	S6

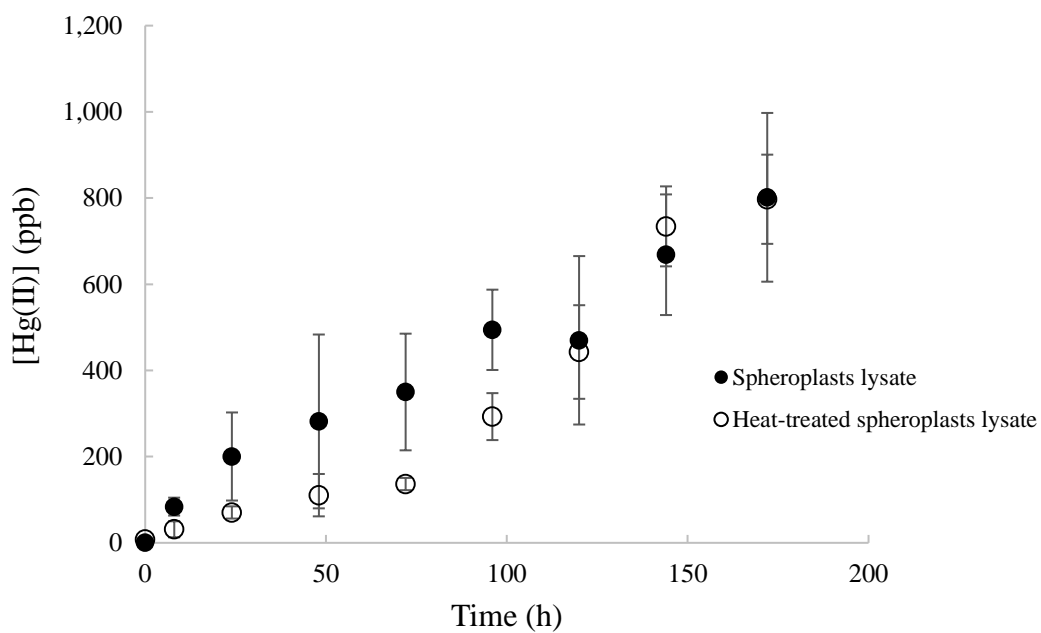
Summary information

Number of pages: 6

Number of figures: 5

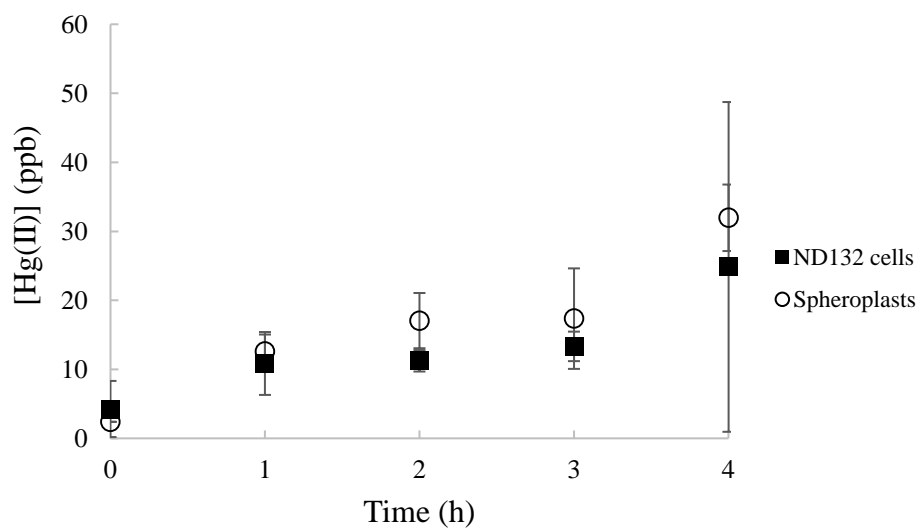
SUPPORTING INFORMATION

Figure S1: Oxidation of Hg(0) to Hg(II) by *D. desulfuricans* ND132 spheroplasts lysate (closed circles) and heat-treated spheroplasts lysate (open circles). Experiments were conducted with an initial cell concentration of 8×10^8 cells/mL. Spheroplasts lysate was treated in 80 °C water bath for 10 min. Points and error bars represent the means and standard deviations of triplicate experiments.



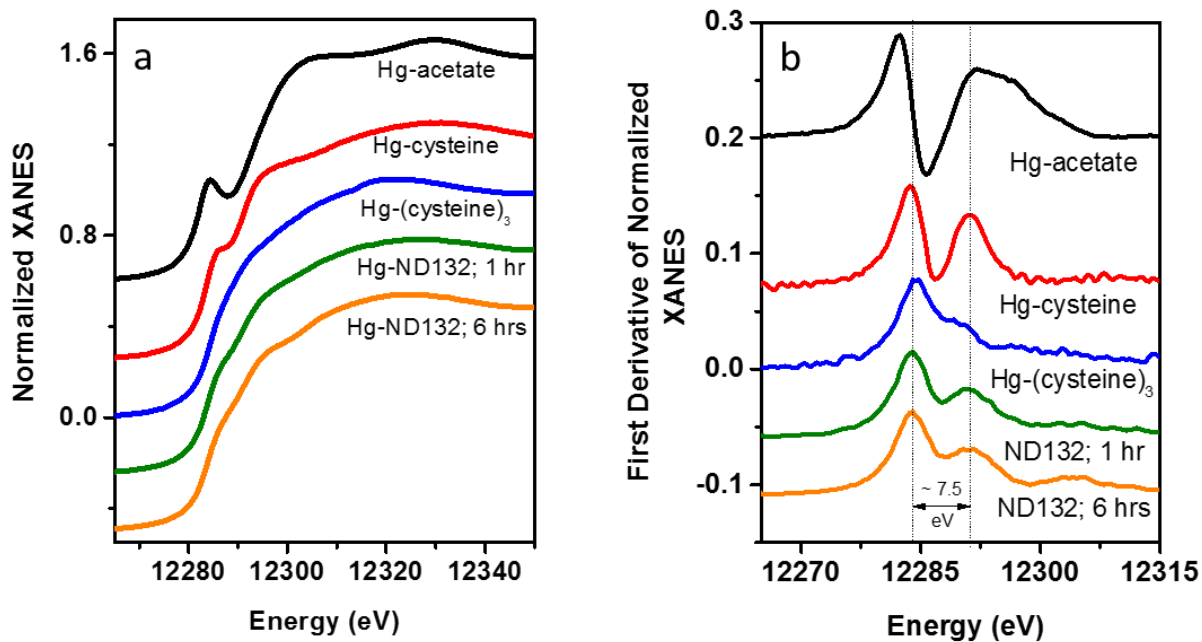
SUPPORTING INFORMATION

Figure S2: Oxidation of Hg(0) to Hg(II) by *D. desulfuricans* ND132 whole cells (closed squares) and spheroplasts (open circles) in sucrose buffer. Experiments were conducted with an initial cell concentration of 8×10^8 cells/mL. Points and error bars represent the means and standard deviations of triplicate experiments.



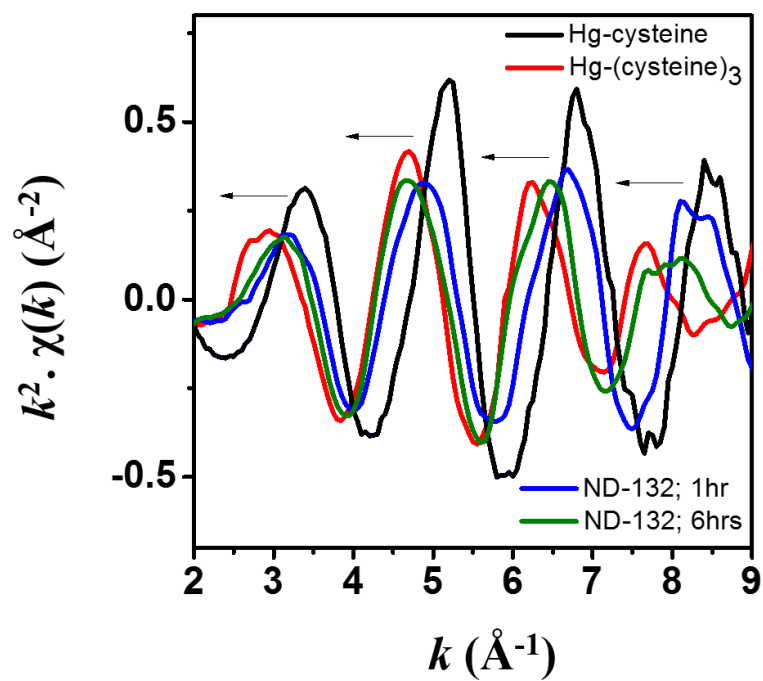
SUPPORTING INFORMATION

Figure S3. XANES spectra of Hg(0)-reacted *D. desulfuricans* ND132 spheroplasts (a) Normalized XANES and (b) first derivative of XANES spectra of spheroplasts samples collected at 1 h and 6 h with Hg-acetate, Hg-cysteine, and Hg-(cysteine)₃ standards.



SUPPORTING INFORMATION

Figure S4: The k^2 -weighted EXAFS spectra in k -space collected on the 1 h and 6 h spheroplasts samples with Hg-cysteine and Hg-(cysteine)₃ standards.



SUPPORTING INFORMATION

Figure S5: (a) Magnitude and (b) real part of the Fourier-transformed EXAFS spectra in R-space of 1 h and 6 h spheroplasts samples with Hg-cysteine and Hg-(cysteine)₃ standards.

